JOURNAL OF OPTOELECTRONICS AND ADVANCED MATERIALS Vol. 10, No. 8, August 2008, p. 2056 - 2060

Fe-catalyzed carbon nanotubes growth on fluidized powders by remote radiofrequency plasma beam

S. VIZIREANU[a], D. STOICA[a], R. BIRJEGA[a], C. GHICA[b], V. TEODORESCU[b], L. NISTOR[b], R GANEA[c], G. DINESCU[a*]
[a]*National Institute for Laser, Plasma and Radiation Physics, Magurele, PO Box Mg36, Bucharest, 077125 Romania*
[b]*National Institute for Material Physics, Magurele, Bucharest, 077125 Romania*
[c]*ZECASIN, Spl. Independentei 202, Bucharest, Romania*

The paper reports the application of a new method combining the Plasma Assisted Chemical Vapour Deposition with the Fluidized Bed Reactor principles for the production of carbon nanotubes on powdered catalysts. An argon plasma beam injected with acetylene in presence of hydrogen was used as fluidized environment for targeting, smashing and mixing the catalytic powder located on the bottom of a cylindrical quartz reactor. The described technique generated plate-like or fibrous like carbon nanostructures on fine Fe particles and carbon nanotubes with 5-10 nm diameters on Fe supported ZSM-5 zeolite.

(Received March 1, 2008; accepted June 30, 2008)

Keywords: Carbon nanotubes, Expanding radiofrequency plasma, Plasma enhanced chemical vapour deposition, Fluidized bed reactor, Fe fine particles, Fe/zeolite ZSM-5

1. Introduction

Many experimental methods were successfully used for the growth of carbon nanotubes (CNTs), as Chemical Vapour Deposition (CVD) [1], Plasma Enhanced CVD [2, 3], Arc Discharge [4] and Laser Ablation [5]. Most of them were used in combination with flat substrates as catalysts. For a large scale production of carbon nanotubes, powdered catalyst and the use of plasma based techniques associated to fluidized bed reactors seems to be the most promising solution. The main advantage of the fluidized bed reactor technique due to the fluidised condition in the quartz tube is the realization of a good contact of the active catalytic species with the precursor gas. However, only a few works on formation of carbon nanotubes on powders via this method can be mentioned [6-10].

We applied the Plasma Assisted Chemical Vapour Deposition method in association with a home made fluidized bed reactor. Argon plasma beam injected with acetylene and hydrogen was used for targeting, smashing and mixing the catalytic powder located at the bottom end of a quartz tube. During the deposition process the powder was kept at 650^{o}C using an external oven. The radiofrequency power injected in the plasma was in the range of 100-300 W and the pressure around 13 mbar, depending on the main Ar flow set up to maintain the flying of the powder in the plasma jet. Different Fe-based pulverulent catalysts, a Fe powder with small particles sizes and Fe-modified zeolite ZSM-5 (Fe/ZSM-5) have been used. We select a zeolite as catalyst support to take benefit of ZSM-5 high specific surface area of around 400 m^2/g and its particular interconnected channels system allowing a good diffusion of reactants.

The catalysts properties were studied by X-ray diffraction (XRD) and the formation and characteristics of carbon deposits were investigated by transmission electron microscopy (TEM).

2. The deposition method

The catalysts were either (1) unsupported Fe fine powders or (2) Fe supported on a ZSM-5 zeolite (Fe-ZSM-5). The Fe-ZSM-5 catalysts were prepared by ion exchange procedure using a parent H-ZSM-5 zeolite and a $Fe(NO_3)_3 \cdot 9H_2O$ solution (ratio solution/zeolite 20 ml/g). The ZSM-5 zeolite was synthesized via a hydrothermal process, assisted by hexandiamine as template, at a Si/Al atomic ratio equal to 50. The as-synthesized zeolite was brought to the H form by the standard procedures. The percentage of Fe in the zeolite is of 1.6 wt %.

The experimental setup, designed for the treatment of powders at high temperatures, uses the principle of fluidized bed reactor. It is presented in Fig. 1.

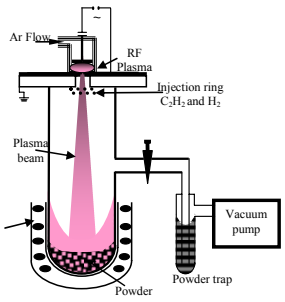

Fig. 1. Diagram of experimental set-up

The plasma jet plays the role of the fluidizing agent. Detailed data concerning the plasma source and its operation principle it is to be found elsewhere [11-14]. The argon (Ar) plasma is remotely generated between two parallel electrodes and expands trough a nozzle into the treatment chamber as a plasma beam. The jet characteristics (size, species) depend on the gas flow rate, pressure and injected radiofrequency power. A mixture of acetylene (C_2H_2) and hydrogen (H_2), was injected in the argon plasma beam through an injection ring. Acetylene serves as carbon species source. Hydrogen was chosen to act as etching agent and inhibiting factor of amorphous carbon phases growth [2, 10], promoting the growth of nanostructured material. The gas flow ratios $Ar/H_2/C_2H_2$, were accurately controlled and measured by mass flow-meter controllers.

The plasma source and the quartz reactor (40 mm diameter and 55 mm length, respectively) are water cooled to prevent the damaging of the gaskets. The bottom part of the reactor where the powdered catalyst was placed is heated for 30-60 minutes up to the reaction temperature of 650^o C, by an external oven. The temperature was kept constant during the experiments. The elements of the home-manufactured fluidized bed reactor can be examined in the picture displayed in Figure 2.

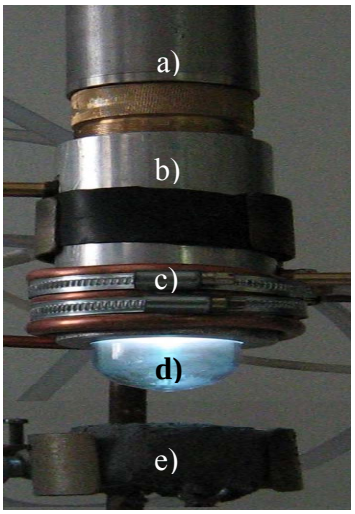

Fig. 2. Picture of the fluidized bed reactor a) plasma generation region, b) source-reactor connection c) reactor cooling system, d) reactor (quartz) tube e) heater (displaced from the region d)

The experiments were performed at 100/8/1 gas flow rates (sccm), while the pressure in the reactor was around 13 mbar and the power injected in the discharge was of 250 W. The experimental protocol consisted of several steps. In a first step, after the powder had been introduced in the reactor, we heated-up under vacuum (10^{-2} mbar) the part of reactor containing the powder. Then, we ignited the plasma in argon with downstream injected hydrogen for oxide reduction and activation of the surface of catalytic powder. After 5-15 minutes, acetylene was injected and the deposition was performed for 30-60 minutes. The last step was the cooling of the sample under Ar flow.

3. Results

The deposition is sustained by acetylene fragments provided by the decomposition of molecules in the main plasma jet, and carried to the bottom part of the reactor, where they target the exposed powder.

The fresh and treated catalysts were studied by X-ray diffraction using a DRON DART 2 UM diffractometer equipped with a Cu-anode and a monochromator in the diffracted beam. The mean crystallites sizes were calculated from the Scherrer's formula $D=k\lambda/(\beta\cos\theta)$, where D is the size, λ is the X-ray wavelength (CuKα), β is the instrumental corrected full width at half-maximum (FWHM), θ is the diffraction angle and the structure factor $k = 0.9$. The results on the fresh and plasma treated powdered catalysts are presented in Figures 3 and 4.

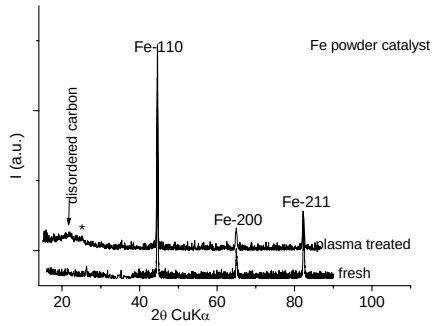

Fig. .3 XRD patterns of fresh and plasma treated, respectively catalyst 2

In the case of Fe fine powder the XRD pattern (Figure 3) shows a well crystallized α-Fe phase. The mean crystallites size obtained by the Scherrer formula is about 42 nm.

The catalyst was pretreated for 10 min in hydrogen plasma at 250 W at a pressure of 13 mbar. The deposition conditions were: gas ratios $Ar/H_2/C_2H_2$ 100/8/1, pressure 13 mbar, RF power 250 W, reaction temperature 650^{o}C and reaction time of 1/2 hour. After treatment the XRD spectrum exhibits the same peaks of an α-Fe phase with a slight broadness indicative of a decrease of a the Fe-crystallites mean sizes to 34 nm, and a broad peak centered around 22.3^o arising from a rather highly disordered amorphous carbon and a very small shoulder around 25^o which could be related to the presence of CNTs. The background is quite higher and disturbed, most likely due to the presence of iron in the amorphous phase.

In the case of another set of experiments, the deposition was performed on Fe supported on ZSM-5 zeolite-matrix of MFI type framework [15]. The MFI framework exhibits a particular structure with a system of perfectly interconnected channels (0.51x0.55 nm and 0.54x0.56 nm) ensuring a high diffusion and selectivity of the reagents during the catalytic reaction. Fe is located in

the cationic positions in the channels, but also very small Fe particles (amorphous to XRD, 5-20 nm in TEM images) can appear as will be shown in the paper section devoted to the TEM results.

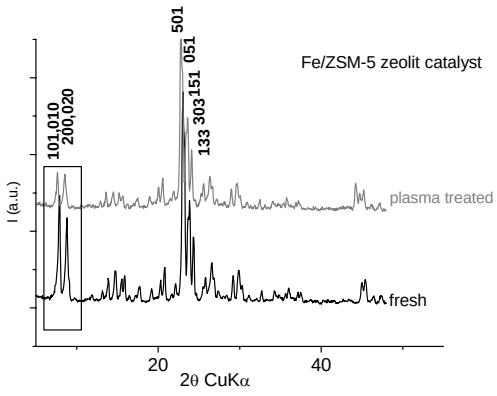

Fig. 4 XRD patterns of fresh and plasma treated, respectively catalyst 3

This catalyst was also pretreated in the same conditions as before. Both patterns of the fresh and plasma treated catalyst, respectively, exhibit the pattern of a MFI framework [16]. In Fig. 4 the typical reflections of the MFI-framework are marked. The XRD pattern of the plasma treated catalysts presents a pronounced decrease of the intensities at low angles with no displacement of the peaks. The low-angles peaks intensities of the MFI framework pattern are particular sensitive to the presence of any species inside the channels [17-20]. The observed decrease of the low-angle intensities is to be attributed to the formation inside the channels system of carbonaceous material, so called "coke" as it was already reported [21]. The preservation of the lattice parameters values upon plasma treatment is indicative of the accommodation of as formed carbonaceous material to the very geometry of the channels.

The plasma treated powder catalysts were investigated by transmission electron microscopy. TEM images were obtained with a JEOL 200 CX electron microscope, operating at 200 kV. The images were recorded with the aid of a Keen View CCD camera. Specimens for TEM observations were prepared by crushing the samples, dispersing the resulting powder in ethanol and dropping it on holey carbon grids.

The TEM images (Fig. 5) of deposited samples of Fe unsupported powder shows iron or iron oxide particles and carbon deposits. The crystalline graphitic carbon forms show two types of morphologies: plate-like (denoted with P) and well crystallized carbon fibers of 500 nm length and 20 nm thickness. In the XRD spectrum no iron oxide could be identified, so we assume the formation of a very thin oxide layered coating on the iron particles.

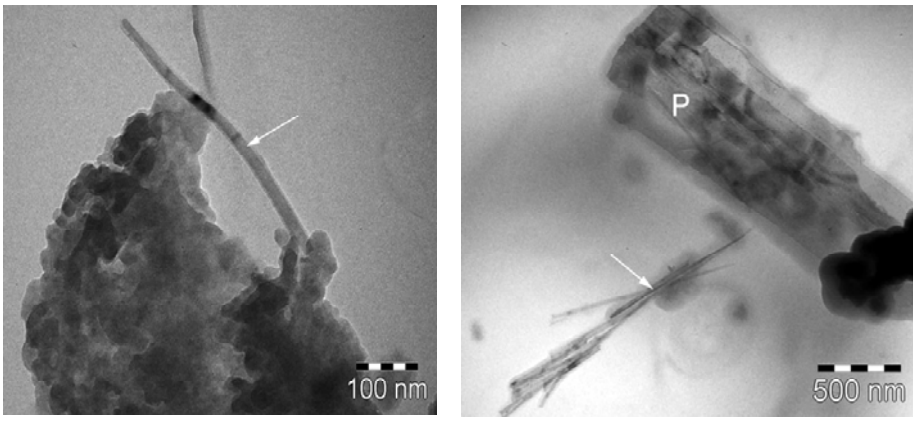

Fig. 5 TEM images of plasma treated Fe powder, showing crystalline carbon fibbers, marked with arrows and crystalline carbon plates marked P

As concerning the ZSM-5 zeolite samples, the TEM images in Fig. 6 show zeolite particles, containing very small (5-20 nm) highly dispersed Fe particles and carbon nanotubes (CNTs) rising from the zeolite. Some of them contain Fe particles at the end. The carbon nanotubes exhibit different morphologies either straight, or curved and even ring-like. They diameter ranges in 5-10 nm.

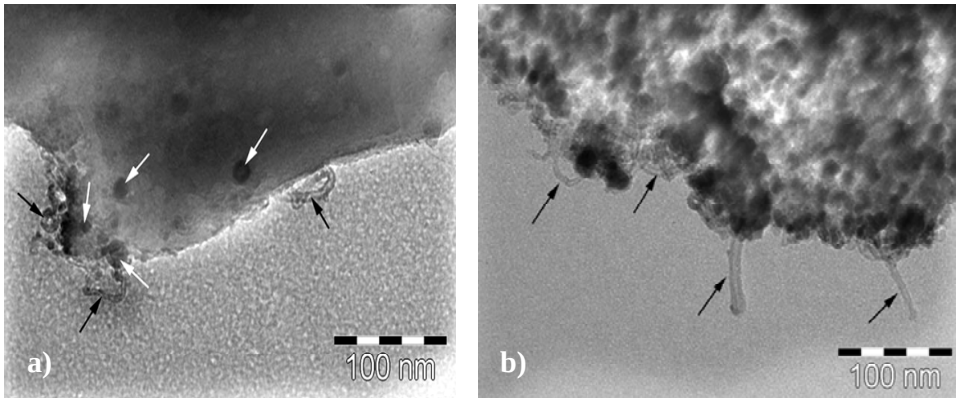

Fig. 6 TEM images of ZSM-5 catalyst after reactive plasma treatment. Carbon nanotubes are formed marked with black arrows. In (a) small, highly dispersed Fe particles are visible and marked with white arrows.

4. Discussion

Our results demonstrate the feasibility of the above described technique to produce nanostructured carbon material and the dependence of the production and morphology of carbon forms on the nature of the catalytic powder used.

On unsupported Fe powder catalyst, containing fine Fe small sized particles, the described technique generated the growth of carbonaceous material with different types or morphologies: plate-like or fibrous-like of large size around 500 nm in length and 20 nm thick.

Genuine carbon nanotubes, 5-10 nm sized, were obtained on highly dispersed and very small sized Fe supported on zeolite. Data concerning the production of carbon nanotubes using zeolites to support metals or metal oxides are few [21-24]. Zeolite Y and $AlPO_4$-5 seems the more effective supports and successful results on a Fe/ZSM-5 catalysts were reported only using the impregnation method [7, 21, 24]. Hernardi et. al [7] had found that zeolite–supported samples prepared by ion-exchange are inactive in the formation of carbons nanotubes which is contrary to our herein reported results. The difference between ion-exchange and the impregnation procedure with respect to the catalytic activity is to be related with the distribution of the metal/metal oxides particles inside the zeolite and/or on their external surface. During an ion-exchange procedure the cationic sites are more homogeneously distributed on the internal surface of the channels in comparison with an impregnation procedure. Upon subsequent calcinations procedures in both cases the metal cations tend to migrate on the external surface of the zeolite crystal with the difference that the ions originating from ion-exchange are more strongly bond to the zeolitic framework and could favour the formation of nanotubes. One should expect to find a large dispersebility and a lower amount of Fe-active species on a Fe ion-exchange zeolite in comparison with a Fe impregnated zeolite, but is most likely that not all the Fe sites are catalytically accessible and active due to the concurrently channels blockage by coke deposits [21]. Probably, our careful approach in the reduction step, by applying a pre-treatment procedure in hydrogen plasma at 250 W at a pressure of 10 torr, activates a larger number of Fe species and maintains at an appropriate dimension the Fe nanoparticles allowing the successful growth of CNTs. The encapsulation of the Fe particles at the end or in the interior of CNTs suggests a hollow nature the tubes. The sizes of nanotubes of 5-10 nm, revealed by TEM analysis, exceeding the MFI framework's channels dimensions account for the formation of CNTs outside the porosity of zeolite. It is with no doubt that Fe nanoparticle with small size and highly dispersed serve as nucleation sites for the growth CNTs [25]. However, it is to bear in mind that the catalytic process is actually more subtle and complex by the fine balance between Fe-catalysts atoms inside the zeolite, precipitated Fe-catalyst atoms on the external surface and Brőnsted sites (bridging hydroxyl) formed by substitution of silicon by aluminum in the ZSM-5 framework. Zeolite as support material for metals catalyst due to its molecular sieve action, their reactive surface implying a stronger interaction of the metal catalysts with support plays a much more important role in the production and control of the morphologies of CNTs.

5. Conclusions

Various methods involving chemical vapour deposition and plasma were successfully used for the growth of carbon nanostructures on catalytic flat substrates. In the case of catalytic powders the deposition process needs peculiar conditions. Fluidized bed reactor is one of the most encouraging methods to be used when powdered catalysts are involved. We report an easy, simply and new technique to produce carbon nanostructures, including carbon nanotubes over catalytic powders using Plasma Enhanced Chemical Vapour Deposition (PECVD) combined with a Fluidized Bed Reactor. The type of carbonic materials formed is sensible different, depending on the nature of Fe-based catalysts: unsupported or supported, particle size, degree of

dispersion. Well crystalline plate-like and fibrous-like carbon (500 nm length and 20 nm thickness) forms were deposited over an unsupported Fe catalyst consisting of small particles and Fe containing amorphous material. Carbon nanotubes of 5-10 nm size were produced over a highly disperse very fine Fe particles supported on a ZSM-5 zeolite.

Acknowledgments

The financial support from the Romanian Ministry of Education and Research received in the frame of CEEX and PNCDI II Research Programmes is highly acknowledged

References

[1] M. Jung, K.Y. Eun, J.K. Lee, Y.J. Baik, K.R. Lee and J.W. Park, , Diam. Relat. Mater. **10**, 1235 (2001).
[2] M Meyyappan, L. Delzeit, A. Cassell and D. Hash, Plasma Sources Sci. Technol. **12**, 205 (2003).
[3] M. Chhowalla, K. B. K. Teo, C. Ducati, N. L. Rupesinghe, G. A. J. Amaratunga, A. C. Ferrari, D. Roy, J. Robertson, W. I. Milne, J. Appl. Phys. **90** (10), 5308 (2001).
[4] S. Iijima, T. Ichisashi, Nature, **363**(6430), 603 (1993).
[5] T. Guo, P. Nikolaev, A. Thess, D. T. Colbert, R. E. Smalley, Chem. Phys. Lett. **243** (1-2), 49, (1995),
[6] Yao Wang , Fei Wei, Guohua Luo, Hao Yu, Guangsheng Gu, Chem. Phys. Lett. **364**, 568 (2002).
[7] K. Hernadi, A. Fonseca, J. B. Nagy, D. Bernaerts, A. A. Lucas, Carbon, **34,** 1249 (1996).
[8] D. Venegoni, Ph. Serp, R. Feurer, Y. Kihn, C. Vahlas, Ph. Kalck, Carbon **40,** 1799(2002).
[9] M. Perez-Cabero, I. Rodriguez-Ramos and A. Guerrero-Ruiz, J. Catal. **215** 305 (2003).
[10] K. Shiji, M. Hiramatsu, A. Enomoto, M. Nakamura, H. Amano, M. Hori, Diam. Relat. Mater. **14**, 831(2005).
[11] G. Dinescu, B. Mitu, E Aldea, M. Dinescu, Vacuum, **56**(1),83-86 (2000).
[12] B. Mitu, S. Vizireanu, C. Petcu, G. Dinescu, M. Dinescu, R. Birjega. Surf. Coat. Tech. 180-181, 238(2004).
[13] S. Vizireanu, B. Mitu, G. Dinescu, Surf. Coat. Tech, **200**, 1132 (2005).
[14] S. Vizireanu, B. Mitu, G. Dinescu, L. Nistor, C. Ghica, A. Maraloiu, M. Stancu, G. Ruxanda, J. Optoelectron. Adv. Mater. **9**, 1649 (2007).
[15] Ch. Baerlocher, W. M. Meier, D. H. Olson, "Atlas of Zeolite Framework Types", Elsevier, Fifth Revised Edition, 184 (2001).
[16] M. N. Treacy, J. B. Higgins, "Collection of the Simulated XRD Powder Patterns for Zeolites, Elsevier, Forth Revised Edition, 234(2001).
[17] A. Araya, B. M. Lowe, Zeolites, **6**, 111 (1996).
[18] X. Liu, J. Klinowski, J. Phys. Chem., **96**, 3403 (1992).
[19] H. Kosslik, V. A. Tuan, B. Parliz, R. Frike, C. Peuker, W. Storek, J. Chem. Soc. Faraday Trans. **89**, 1131 (1993).
[20] B. F. Mentzen, M. Sacerdot-Peronnet, J. –F. Berar, F. Lefebvre, Zeolites, **14**, 485 (1993).
[21] K. Hernardi, A. Fonseca, J. B. Nagy, D. Bernaerts, A. Fudula, A. A. Lucas, Zeolites, **17**, 416-423 (1196).
[22] J. Rodriguez-Mirasol, T. Cordero, L. R. Radovic, J.Rodriguez, Chem. Mater., **10** 550 (1998).
[23] G. D. Li, Z. K. Tang, N. Wang, K. H. Wong, J. S. Chen, Stud. Surf. Sc. Catal. **135**, 21P0 (2001).
[24] A. M. Zhang, Q. H. Xu, J. J. Zhao, J. M. Cao, Stud. Surf. Sc. Catal. **135**, 22P08 (2001).
[25] J-B. Park, G.-S. Choi, Y.-S. Cho, S.Y. Hong, D. Kim, S.-Y.Choi, J. L.Lee, K. I. Cho, J. Cryst.Growth, **244** 211 (2002).

*Corresponding author: dinescug@infim.ro